Wavelet Packet Transform Based Compression for Bilateral Teleoperation

Journal:	*Part I: Journal of Systems and Control Engineering*
Manuscript ID:	JSCE-14-0060.R1
Manuscript Type:	Special Issue
Date Submitted by the Author:	n/a
Complete List of Authors:	Kuzu, Ahmet; TUBITAK, BILGEM; Istanbul Technical University, Control&Automation Eng Baran, Eray; Sabanci University, Faculty of Engineering and Natural Sciences Bogosyan, Seta; UAF, ECE Gokasan, Metin; Istanbul Technical University, Control Engineering Deparment Sabanovic, Asif; Sabanci University, Faculty of Engineering and Natural Sciences; Sabanci University
Keywords:	controller and system design methods, real time systems, information management, direct drive robots, systems modelling
Abstract:	This paper introduces a codec scheme for compressing the control and feedback signals in bilateral control systems. The method makes use of Wavelet Packet Transform (WPT) and Inverse Wavelet Packet Transform (IWPT) for coding and decoding operations respectively. Data compression is carried out in low pass filter output by reducing the sampling rate; and in high pass filter output by truncating the wavelet coefficients. The proposed codec works on both directions of signal transmission between a master robot and a slave robot over a networked motion control architecture. Following the formulation of the compression/decompression methodology, experimental validation is conducted on a single degree of freedom (DOF) motion control system. In the experiments, responses from different Wavelet structures are analyzed and a comparative study is carried out considering the factors of compression rate, reconstruction power error and real time computational complexity. It is confirmed that the controller using the proposed compression algorithm performs very close to the uncompressed one while enabling transmission of much less data over network.

Wavelet Packet Transform Based Compression for Bilateral Teleoperation

Ahmet Kuzu*†, Eray A. Baran‡, Seta Bogosyan§*, Metin Gokasan*, Asif Sabanovic‡

*Istanbul Technical University, Istanbul/TURKEY, {kuzuah,gokasan}@itu.edu.tr
†*(Corresponding Author)* Tubitak, Bilgem, Kocaeli/TURKEY, ahmet.kuzu@tubitak.gov.tr
‡Sabanci University, Istanbul/TURKEY, {eraybaran,asif}@sabanciuniv.edu
§University of Alaska, Alaska/USA, sbogosyan@alaska.edu

***Abstract*—This paper introduces a codec scheme for compressing the control and feedback signals in bilateral control systems. The method makes use of Wavelet Packet Transform (WPT) and Inverse Wavelet Packet Transform (IWPT) for coding and decoding operations respectively. Data compression is carried out in low pass filter output by reducing the sampling rate; and in high pass filter output by truncating the wavelet coefficients. The proposed codec works on both directions of signal transmission between a master robot and a slave robot over a networked motion control architecture. Following the formulation of the compression/decompression methodology, experimental validation is conducted on a single degree of freedom (DOF) motion control system. In the experiments, responses from different Wavelet structures are analyzed and a comparative study is carried out considering the factors of compression rate, reconstruction power error and real time computational complexity. It is confirmed that the controller using the proposed compression algorithm performs very close to the uncompressed one while enabling transmission of much less data over network.**

***Index Terms*—Bilateral Control, Teleoperation, Wavelet Packet Transform, Haptic Data Compression**

I. Introduction

Recent achievements of robotics technology paved the way through control of multiple robotic systems to accomplish certain tasks together. Teleoperation, referring to the operation from a distant location, is an example of bilateral control structure between distant robotic systems. Due to its potential contribution on the applications including safety, security, exploration and biomedical sciences, teleoperation systems recently became an active research field. Some examples including the use of robotic systems with bilateral control include hazardous area explorations, chemical material deposition systems, telesurgery and aerospace applications. The main problem of a bilateral control system is to provide synchronized control of positions and forces between geographically separated motion control systems. Especially when internet medium is used for data exchange, communication delays between the transmitted signals make the motion synchronization problem further difficult.

Signal transmission over internet causes problems such as deterioration of stability and controller performance. The problem arise due to the limitations of network communication and existence of time delay in the internet medium. Providing robust operation in a bilateral control system can be feasible only after communication constraints are taken into consideration [1]. Besides the effect of time delay, conflicting nature of bandwidth limitations and sampling rate have direct consequences on the performance of the controller and vivid haptic sensation from the remote environment [2].

In the literature, several studies have been proven to perform successfully for teleoperation systems. One of the early studies about time delay problem proposed the use of Smith Predictor for compensation of the motion in the existence of constant and known amount of delay [3]. A relatively modern approach is adopted by methods utilizing passive signal exchange [4], [5], [6] and methods based on scattering theory and wave variables [7]- [8]. Some recent studies based on impedance adaptation have been shown to perform successful for better reconstruction of interaction forces of unstructured remote environments on the master side [9], [10]. The stability proofs of these methods have been studied in various settings. However, most of these methods still lack in terms of transparency, which is a must in teleoperation systems [11]. Besides the solutions using passivity theory and wave variables, methods based on the concept of network disturbance have also been popularized for applications on teleoperation systems [12], [13], [14]. Studies considering the solution of time delayed motion synchronization problem from a robust acceleration control point of view have been proposed in [15] and [16].

In order to quantify the performance of teleoperation systems, some researchers defined certain metrics mostly based on telepresence and transparency [17]. Based on such indices, quantitative and analytical comparisons of some of the methods used for motion control under time delay are presented in [18] and [19]. For further information, reader is addressed to the recent survey given in [20].

One of the major factors that affect the performance of a bilateral control algorithm is the loop execution frequency. The fact from Nyquist theory implies that the shorter sampling period yields the wider bandwidth of the signal [21]. The communication infrastructure of a teleoperation system, having consisted of communication lines and rooter devices, imposes significant limitations on packet transmission rates. Moreover, as a natural drawback of internet medium, network

congestion risk increases when an interval of packet transmission is shortened. Because of network congestion, amount of communication delay and rate of packet loss increase significantly, which deteriorates the performance of overall control system. In order to overcome the effects of congestion, some compression based methods have been proposed that set the frequency of packet transmission lower than that of the control loop [2], [22], [23]. Utilization of compression algorithms implies the existence of two Nyquist frequencies for the acquisition of a signal; one that is determined by the sampling period for the control, and the other being determined by the packet transmission rate.

Similar kind of problem can be observed in biomedical sciences when trying to transmit bio-potential signals, such as electrocardiogram (ECG) data, over the network. For those systems, compression schemes are used that implicitly make use of some transformations. Some examples of these compression structures include the discrete cosine transform (DCT), Walsh transform, Karhunen-Loeve transform (KLT), and wavelet transform. The contribution made by using a transformation for compression comes from the ability to concentrate the energy of the original signal in smaller sized data packages. With particular selection of the transformation scheme, it becomes feasible to represent the signal by using small number of coefficients in exchange of small losses from the original data [24]. In that sense, mappings that would contain more of the energy from the original signal in smaller sized samples would perform better for the compression. The wavelet transform has a good localization property both in time and frequency domains and fits this purpose of the compression idea. Furthermore, by appropriate selection of the wavelet function, representation of the same signal can be obtained with smaller error.

Despite being an important factor influencing performance, the use of compression approaches in the area of teleoperation and bilateral control are very rare [25], [26], [27] and are mostly based on DFT and DCT. The novel WPT codec scheme approach proposed by the authors was demonstrated to have a better performance over those approaches in the literature with its capability to track the original signal even at $\%90$ compression rate. [28] This is an improved performance over existing compression approaches in the literature: In [29], the DFT approach was demonstrated by the authors to have a better performance over DCT, and yet to diverge even at $\%80$ compression rate, [28]. Besides its significantly improved performance, another advantage of the proposed WPT approach is its increased flexibility, which allows for a higher number of parameters to be adjusted, i.e. wavelet type, wavelet buffer, vanishing moments, and wavelet level, in comparison to DFT's single adjustement parameter, which is buffer length.

The main contribution of this study is a detailed performance analysis and experimental verification for the author's WPT approach [28] proposed for teleoperation and bilateral control applications. To this aim, different wavelet families have been analyzed and experimentally tested at different buffer lengths, wavelet levels, and compression rates, also considering computational cost. The analysis is based on the teleoperation system which was also used in the evaluation of the DFT and DCT approaches in the authors' previous papers [28] and [29].

The organization of the paper is as follows. Section II describes the general scope of bilateral control system and bandwidth problem along with an exiting method used for compensation of time delay. Section III introduces the Wavelet Packet Transform while in Section IV, most commonly used basis functions of Discrete Wavelet Transform (DWT) are summarized. Section V discusses the WPT based compression/decompression idea utilized for bilateral control. Finally, in Sections VI, VII and VIII, results acquired from the experimental case studies, analytical discussion over experiment results and concluding remarks are presented respectively.

II. Bilateral Control And Bandwidth Problem

Bilateral control refers to the control of a master-slave structure based robotic system in order to synchronize the position and force responses of the robots used within. In a bidirectional flow manner, the position information of the master robot is sent to the slave robot as reference while the force measured on the remote (i.e. slave) side is fed back to the master robot to provide interaction with the operator. Teleoperation, in that context, refers to the process of operation in a distant location. Having mentioned about a remote environment, one major problem in bilateral control is the difficulty of satisfying motion synchronization requirement via data transmission over the internet. The conventional structures of data transmission contain the use of protocols like UDP/IP and TCP/IP which are subject to transmission delays of unpredictable magnitude. Under these conditions, the control problem takes the form of a variable time delay impedance control problem, which is even a more challenging one than the static time delay control problem.

When network within the control loop is taken into consideration, the trade-off between bandwidth and sampling starts to play a more important role in the system. The uncertain and unstructured form of network medium can yield problems related to variable magnitude transmission delays, or in certain settings of the network (like UDP/IP), problems due to package losses. For such circumstances, reducing the sampling rate of data sent through network can improve the performance by reducing the delays and package losses in the loop. However, in order to maintain stable operation, high frequency sampling is inevitable for the overall control system. Especially, rapidly changing signals like the input current or reaction force measurement is affected negatively from lowered sampling frequency, which results in degradation of performance for the entire control loop. One good example of performance loss can be seen while having force measurements for hard-contact (i.e. interaction between environments with high stiffness) force control operation.

In order to solve the conflicting behavior of sampling ratios within the system, researchers proposed to use compression/decompression (codec) algorithms for data transmission

over the network [21], [30]. Benefiting from codec structure, one can increase the loop frequency of the control system while preserving the data transmission frequency at respectively low values. The new scheme presented in the context of this paper is based on this down sampling idea and uses WPT based compression scheme. Below, a brief overview of the controller used for the verification of the proposed algorithm is presented.

The time delayed motion control algorithm utilized for this study makes use of the concept of network disturbance and is based on the controller structure presented in [14], namely the Communication Disturbance Observer (CDOB). In CDOB structure, the effect of delay in the measurement channel is lumped under the term network disturbance which acts in the acceleration dimension. Hence, in the background, the master and slave plants implicitly makes use of acceleration control framework. Below a brief overview of the system and controller used in this study is presented.

A. System Definition

In the following analysis, the demonstration of the system and corresponding controller will be made on a single degree of freedom (DOF) system. Without loss of generality, one can represent the dynamics of a single-DOF system as;

$$a_n \ddot{q}(t) = \tau(t) - \tau_{dis}(t) \tag{1}$$

where, a_n and $\tau_{dis}(t)$ respectively stand for the nominal plant inertia and disturbance torque acting on the plant for which generalized coordinate of motion is represented by $q(t)$. Assuming small variations around the linear region, one can write down the input torque as a scalar multiple of the input current and nominal torque constant (i.e. $\tau(t) = K_n i_c(t)$). Substituting this back to equation (1) gives the following

$$a_n \ddot{q}(t) = K_n i_c(t) - \tau_{dis}(t) \tag{2}$$

In equation (2), the term τ_{dis} combines all undesired effects, namely the viscous friction ($b(q, \dot{q})$), deviations from the nominal values for torque constant (ΔK_n) and inertia (Δa_n), effect of gravity ($g(q)$) and all other external torques (τ_{ext}) acting on the system. Hence, the content of $\tau_{dis}(t)$ can be given as;

$$\tau_{dis} = \Delta a_n \ddot{q} + \Delta K_n i_c + b(q, \dot{q})\dot{q} + g(q) + \tau_{ext} \tag{3}$$

In order to use the plant in acceleration control framework, one has to estimate and compensate the disturbance term given in (3). The realization of this ideal behavior can be acquired via the integration of a Disturbance Observer (DOB) with the remote plant [31] either alone, or with additional compensation if further precision is required [32].

B. Motion Compensation with Time Delay

When there is delay in either or both of control and measurement channels, real time signal transmission is hindered. Especially due to the delays in measurement channel, the controller cannot acquire the information of the remote system states and hence cannot generate necessary and correct control input on time which leads an unstable behavior. Further, additional delay in the control channel also contributes negatively on the synchronized motion of master and slave systems [33]. The stable operation of the controller can only be acquired if correct estimates of the remote system states can be done. The estimation structure used in the context of this study is the Communication Disturbance Observer (CDOB) presented in [14]. In CDOB structure, the effect created by the measurement delay is considered as a disturbance in acceleration dimension which can be modeled as;

$$\tau_{dis}^{nw}(t) = K_n i_c(t) - a_n \ddot{q}_s(t - D_m) \tag{4}$$

where $\tau_{dis}^{nw}(t)$ represents the network disturbance, D_m stands for the delay in the measurement channel, $q_s(t)$ represents the remote system (i.e. slave system) position and $i_c(t)$ represents the control current sent from the master side over network. The observer implicitly assumes that the slave plant is enforced to behave ideal with nominal torque constant K_n and nominal inertia a_n via a disturbance observer as explained in the previous section. Having assumed the nominal behavior of the remote system, the network disturbance can be estimated with another DOB which is termed as the Communication Disturbance Observer due to obvious reasons.

The estimated network disturbance stand for the torque that is supposed to act on the slave plant during measurement delay. Since the remote plant is enforced to behave nominal with DOB, the estimated network disturbance can be divided by the corresponding nominal inertia and be integrated to give the velocity difference that is supposed to exist during the measurement delay time. Mathematically, we have;

$$\Delta \dot{q}_s(t) = \frac{1}{a_n} \int_0^t \tau_{dis}^{nw}(\varphi) d\varphi \tag{5}$$

Addition of this velocity difference to the delayed slave velocity gives the estimated velocity of the slave plant as shown below

$$\hat{\dot{q}}_s(t) = \dot{q}_s(t - D_m) + \Delta \dot{q}_s(t) \tag{6}$$

The depiction of CDOB structure is given in Fig. 1 below. Further information about CDOB can be found in [12] and [13], whereas a convergence and stability analysis is given in [15].

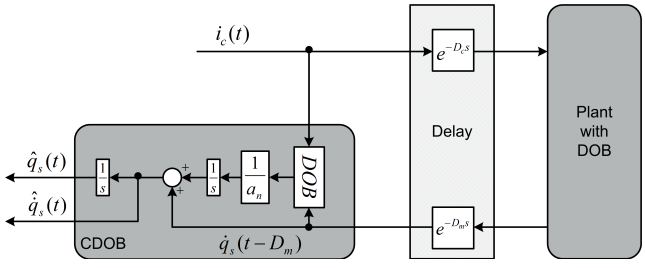

Fig. 1. Structure of Network Controller

The system compensated with the CDOB structure exhibits a stable behavior with the estimation of the real time slave

motion measurement. In other words, CDOB converts the overall system to one without the measurement delay. Using the estimation from CDOB, the master side controller can generate the necessary input reference that is supposed to act on the slave system after the input channel delay.

III. Wavelet Packet Transform

In time-series, analysis can be handled by either in time domain perspective such as moments and correlations or can be handled in the frequency domain perspective such as energy spectra of signals. Wavelets yield a way to analyze these signals both in time and frequency domains by producing local spectral information about them [34]. Unlike the Fourier based waves, which covers the whole time axis, wavelets are localized in a bounded interval of time which satisfies a few requirements. This elasticity enables construction of new wavelets for new applications. The information from which the signal can be a analyzed and reconstructed in the selected time and frequency span can be contained in the wavelet coefficients. Due to their advantages in providing local information, wavelets have been adopted to perform efficiently in many applications like identification and estimation [35].

Wavelets are defined by the wavelet function $\psi(t)$ also called the mother wavelet and scaling function $\phi(t)$ also called the father wavelet in the time domain. From a practical point of view, wavelet function acts like a band-pass filter with scaling. Hence, in order to cover the entire signal spectrum, one has to use an infinite number of wavelets. Mathematically speaking, the fundamental form of wavelets can be given as follows;

$$\psi(t) = \sqrt{2}\sum_{n\in\mathbb{Z}} g(n)\phi\left(2t-n\right) \tag{7}$$

$$\phi(t) = \sqrt{2}\sum_{n\in\mathbb{Z}} h(n)\phi\left(2t-n\right) \tag{8}$$

where, $g(n)$ and $h(n)$ stand for the high pass and low pass filters respectively which, together constitute a pair of conjugate quadrature filters [36].

Application of wavelets on practical systems is very similar to the realization of sub-band coders. In this approach, the signal is separated into low and high frequency parts that are called approximation and detail respectively. In 1988, Mallat produced a fast wavelet decomposition and reconstruction algorithm [37]. The Mallat algorithm for Discrete Wavelet Transform (DWT) is a two channel sub-band coder which uses conjugate quadrature filters (CQFs) or quadrature mirror filters (QMFs). The one-level DWT algorithm, which is usually denoted as the decomposition algorithm, is shown in Fig. 2 below.

Here, LDF denotes low pass decomposition filter and HDF denotes high pass decomposition filter which are orthogonal to each other, c_A denotes approximate wavelet coefficients and c_D denotes detailed wavelet coefficients. We will call this one-level discrete wavelet transform in the rest of the paper as DWT1.

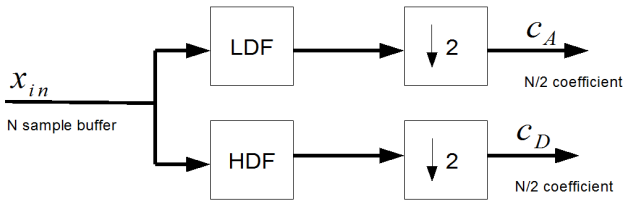

Fig. 2. Wavelet Decomposition Algorithm

The inversion of the process is similar to the forward case and can be done by just exchanging down-sampling to up-sampling and quadrature filters to quadrature mirror filters as shown in Fig. 3.

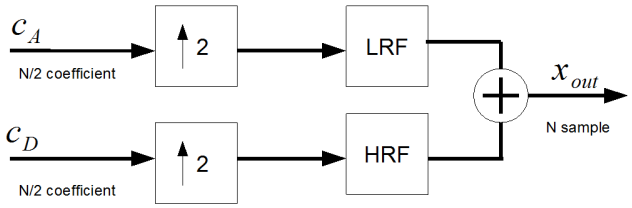

Fig. 3. Wavelet Reconstruction Algorithm

Here, LRF and HRF represent the low-pass reconstruction filter and high pass reconstruction filter respectively, which are again orthogonal to each other. Similar to the forward case, this one level inverse discrete wavelet transform will be abbreviated as IDWT1 in the context of this paper.

IV. DWT Basis Functions

In wavelet transform, the acquisition of information localized within the signal is dependent on the selection of the basis functions (i.e. wavelets). Based on the structure hidden in the basis function, the information is retrieved via dilations and shifting operations. Hence, it is important to decide on the correct wavelet for particular type of application since some basis functions might reveal deeper content from the same signal. For convenience of the reader, we provide below a brief summary of the most commonly used DWT basis functions. The derivations and construction procedures of these wavelets require a much deeper discussion, which is beyond the scope of the work presented here.

A. Haar

Haar wavelet family is combination of a sequence of square shaped functions scaled to construct a basis for transformation [38]. This family constitute the simplest possible wavelets that exists in the literature and can be shown to be a special case of Daubechies wavelet (i.e. D2). The Haar family wavelets are not continuous and therefore are not differentiable which provide advantage in analyzing suddenly changing signals. The mother function $\psi(t)$ and the corresponding scaling function $\phi(t)$ for the Haar wavelet family can be given as follows;

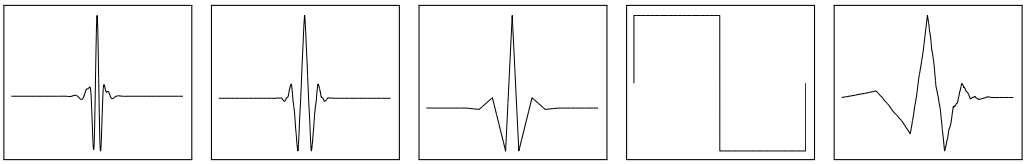

(a) coif5 (b) bior2.6 (c) rbior2.6 (d) haar (e) db3

Fig. 4. General Shapes of Wavelet Basis Functions

$$\psi(t) = \begin{cases} 1 & 0 \leq t < 1/2 \\ -1 & 1/2 \leq t < 1 \\ 0 & \text{otherwise} \end{cases} \tag{9}$$

$$\phi(t) = \begin{cases} 1 & 0 \leq t < 1 \\ 0 & \text{otherwise} \end{cases} \tag{10}$$

B. Coiflets

Coiflets constitute another set of discrete wavelet basis functions which have scaling functions with vanishing moments [39]. Vanishing moments are the degrees of the polynomials representing a linear combination of the smoothing function and its translation. It determines the convergence rate of wavelet approximation. Mathematically, the mother and scaling functions of generalized Coiflet of order l (denoted as $\psi_{l,\mu}$ and $\phi_{l,\mu}$) for some $\mu \in \mathbb{R}$, is supposed to satisfy;

$$\int_{\mathbb{R}} t^p \psi_{l,\mu}(t) dt = 0 \tag{11}$$

$$\int_{\mathbb{R}} (t-\mu)^p \, \phi_{l,\mu}(t) dt = \delta_p \tag{12}$$

where, $p = 0, 1, ..., l-1$ and μ is the center of mass of scaling function $\phi_{l,\mu}(t)$ [36].

C. Daubechies

Daubechies family constitute an orthogonal wavelet basis which is characterized by a maximum amount of vanishing moments for some given support N. These wavelets are widely used for analysis of self similarity or signal discontinuity problems. An easy way to realize Daubechies wavelets practically is to make use of Fast Wavelet Transform [40]. Unlike other wavelets, in Daubechies wavelets the mother function is dependent on the scaling function and the scaling function can be obtained from a recursion equation [41]. Mathematically, for $N \in \mathbb{N}$, Daubechies wavelet of class D-$2N$ can be obtained from the following mother and scaling functions;

$$\psi(x) = \sqrt{2} \sum_{k=0}^{2N-1} \left(-1^k\right) h_{2N-1-k} \phi\left(2x-k\right) \tag{13}$$

$$\phi(x) = \sqrt{2} \sum_{k=0}^{2N-1} h_k \phi\left(2x-k\right) \tag{14}$$

where, $h_0, h_1, ..., h_{2N-1}$ are the constant coefficients of filter satisfying the following conditions;

$$\sum_{k=0}^{N-1} h_{2k} = \sum_{k=0}^{N-1} h_{2k+1} = \frac{1}{\sqrt{2}} \tag{15}$$

$$\sum_{k=2l}^{2N-1+2l} h_k h_{k-2l} = \begin{cases} 1 & \text{if } l = 0 \\ 0 & \text{if } l \neq 0 \end{cases} \tag{16}$$

with $l = 0, 1, ..., N-1$. As obvious from equation (13), in order to obtain the wavelet, first the recursion given in equation (14) has to be solved for $x \in \mathbb{R} \backslash [0, 2N-1[$.

D. Bior

The Biorthogonal wavelet family differs from the function side since they are not based on vanishing moments [42]. Although they are very different from the Daubechies wavelets in terms of shape and properties, their construction idea is exactly same. Moreover, all generators and wavelets in this family are symmetric. Mathematically, the form of the corresponding mother and scaling functions [43] for Bior wavelet family can be given as;

$$\psi(t) = \sum_{k=0}^{N} 2g^r(k) \phi\left(2t-k\right) \tag{17}$$

$$\phi(t) = \sum_{k=0}^{N} h^r \phi\left(2t-k\right) \tag{18}$$

where, $g^r(k)$ and $h^r(k)$ stand for the reverse of the original filters $g(k)$ and $h(k)$ respectively.

E. Rbior

Reverse Biorthogonal wavelet functions are generated by interchanging decomposition and reconstruction filters of the original Biorthogonal wavelet functions. The mother and scaling functions of these wavelets share the same mathematical representation with the original Biorthogonal wavelets as given in equations (17) and (18) respectively. Rbior wavelets are widely used for system identification.

The variations between the wavelet functions result in differences in terms of compression rates and computational complexities introducing a pay-off to select the best wavelet function for the particular application in hand. The dependency of compression rate is more closely related to the shape of the signal being compressed and the shape of the wavelet used for the transformation. On the other hand, having chosen a particular wavelet structure for application, problems related

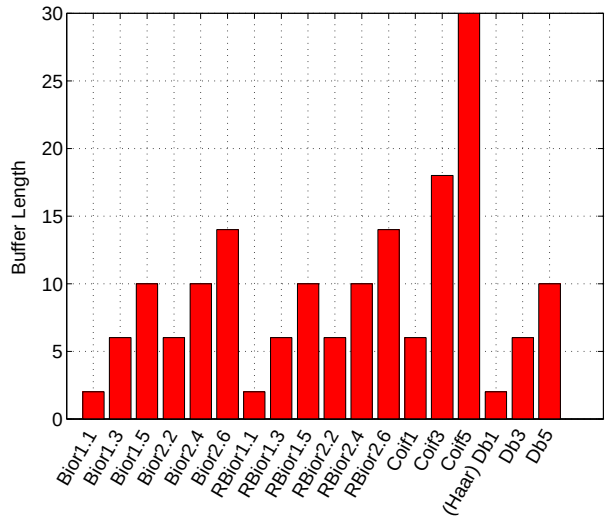

Fig. 5. Filter Length of Wavelets

to computational complexity may come into picture based on the selected vanishing moment, buffer size and compression level. In order to provide a consistent analysis of the selected wavelets, the general shapes of these wavelets and the information related to their buffer sizes are provided in Fig. 4 and Fig. 5 respectively.

V. WPT Based Compression System for Bilateral Control

The wavelet packet method involves decomposing the signal using wavelets in binary tree form. For the selected orthogonal wavelet function (LDF and HDF), we generate a set of bases called wavelet packet bases. Every set has particular features of the original signal. The wavelet packets can be used for lots of expansions of a given signal.

In the orthogonal wavelet decomposition procedure, the approximation coefficients are always separated into two parts, resulting in a vector of approximation coefficients and a vector of detail coefficients, both of which work at a coarser scale. Then, the approximation coefficient vector is separated again, but details are not reanalyzed anymore. Hence, the information loss is in the detailed side. In case of wavelet packet transmission, both detail and approximation coefficient vectors are separated, hence offering the richest analysis capability. The complete binary tree is produced in this way as given in the Fig. 6 (A) and (B) below.

In the WPT based compression architecture, wavelet packet tree system is used to decompose and reconstruct the signal. Once again, the signal is separated into its low and high frequency parts. Following this separation, the low frequency component of the signal is down-sampled and the high frequency component of the signal is compressed according to algorithm which saves the predefined amount of maximum wavelet component and cancels others.

For the decompression process, the low frequency part and high frequency components are decompressed separately and

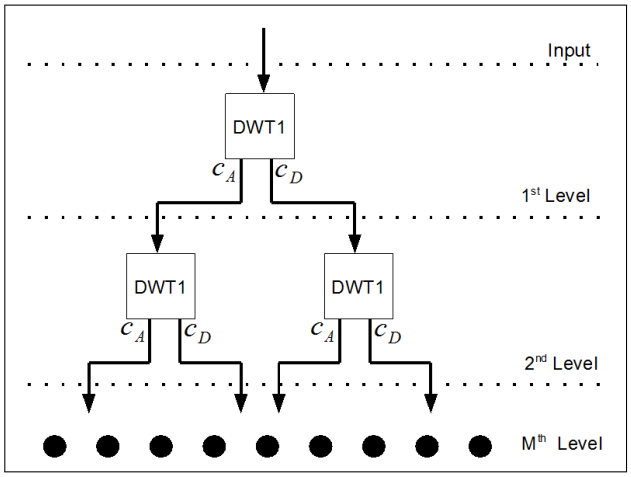

(A)

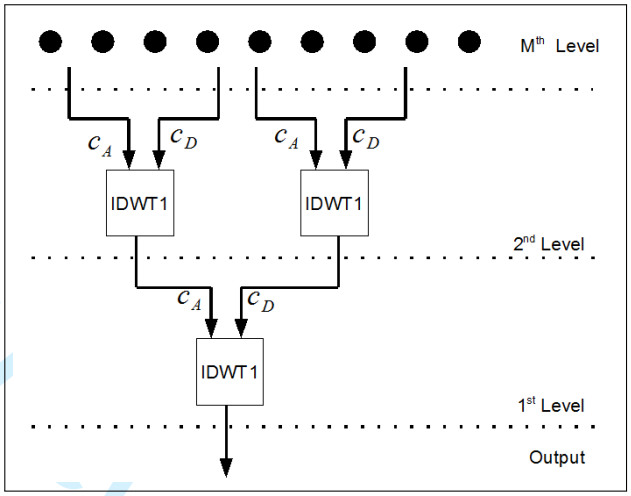

(B)

Fig. 6. Wavelet Packet Transform Tree; (A) Decomposition, (B) Reconstruction

then combined together. It is adequate to hold each sample of low frequency signal for N times. For decompression of the high frequency side, the inverse wavelet packet transform is applied to the wavelet packet tree. The selection process means saving maximum predefined amount of components. Having acquired the two components constituting the original signal, low frequency components are summed with decompressed high frequency signals and the recovery of the original data is completed. The whole process is shown in Fig. 7.

VI. Experimental Results

The experimental validation for the proposed compression scheme is performed on an experimental setup including linear direct drive motors used for the realization of bilateral control. The experimental platform consisted of two Hitachi-ADA series linear AC motors and drivers equipped with Renishaw RGH41 type incremental encoders that has $1\mu m$ resolution.

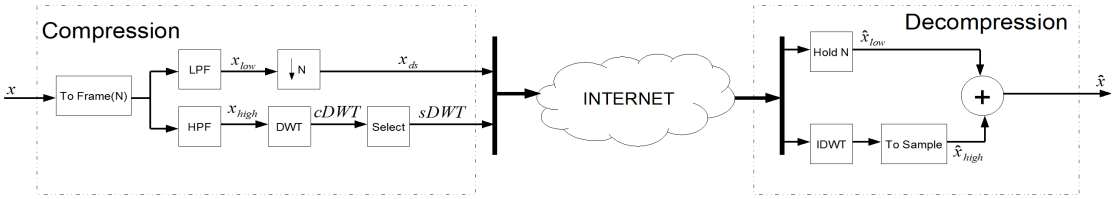

Fig. 7. Proposed DWT Based Compression-Decompression Scheme

The algorithm is compiled from a C code and real time processing is executed by a D-Space DS1103 card.

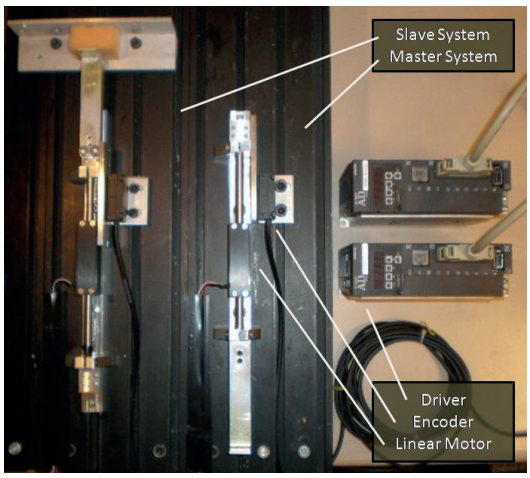

Fig. 8. Experimental Setup

In the experiments, artificially generated time delays that have constant and varying components in both measurement and control channels are employed between master and slave operators. During experiments, the compression and decompression is made using the WPT based compression algorithm running in various parameter sweep conditions to test their effects on the overall performance. These conditions include wavelet family, compression level (i.e. depth), buffer size and compression ratio. A picture of the experimental setup is given below in Fig.8.

In the experiments, the master operator is computer controlled with sinusoidal position reference and the corresponding control current $i_c(t)$ from the same sine position tracking command is used in the compression algorithm since in bilateral control current of the master system is the primary data that is sent to the remote system. Selection of the input current has one more important aspect. Since current input is the fastest varying signal within the control loop (i.e. the signal for which high frequency components carry the most important information) the performance of the compression algorithm can best be seen on this data. Fig. 9 shows one segment of the compressed control current while the detailed plots obtained by zooming on the marked region is provided over the same figure.

In order have better evaluation of performance, power

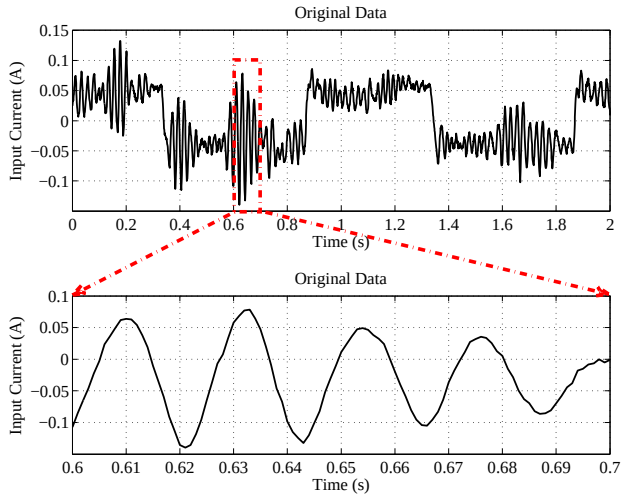

Fig. 9. Original Signal Used for Compression-Decompression

error comparisons are made using the same signals for every different scenario. For each case, the compression ratio is changed from %0 to %100 and the results are plotted with respect to the following power error E_P;

$$E_P = \frac{P_{Original} - P_{Decomposed}}{P_{Original}} \times 100 \qquad (19)$$

where, $P_{Original}$ and $P_{Decomposed}$ respectively stand for the power of original and decomposed signals.

Since the number of parameters that affect the overall algorithmic performance are relatively high, here we adopt a methodological way to observe the effects of these parameters by carrying out separate analysis for each different factor. For that purpose, three different experiment sets are carried out and explained below.

A. Experiment Set-1

The first experiment set covers analysis with respect to the wavelet family and compression depth for which the results are given in Fig. 10. In these figures, the main objective is to see the change in responses via changing the vanishing moments of the corresponding family and changing the compression depth (i.e. level) under constant vanishing moment of the corresponding family. The families used in the experiment content include Biorthogonal 1.x, Biorthogonal 2.x, Reverse Biorthogonal 1.x, Reverse Biorthogonal 2.x, Coiflets and

Daubechies, given in Fig 10-(a), Fig 10-(b), Fig 10-(c), Fig 10-(d), Fig 10-(e) and Fig 10-(f) respectively. In these figures, for each family, upper subfigure shows the effect of family parameter on power error with respect to comparison ratio and lower subfigure shows the effect of wavelet depth on power error with respect to comparison ratio.

Referring to the upper subfigures, one can conclude that the compression error decrease slightly with increasing vanishing moments for every wavelet family. On the other hand, the computational complexity comes into picture when talking about increasing vanishing moments since that means increasing the length of reconstruction and decomposition filters as seen in Fig. 5. Hence, one has to take into consideration the relative change in the required computational power for a small enhancement in the compression performance.

On the other hand, having observed the lower subfigures, one can deduce that increasing the wavelet depth results in better performance regardless of the wavelet structure. This result is consistent with the intuitional expectation, since at every additional level more coefficients are generated to represent the same signal. However, here again one has to consider the increasing computational complexity with the increasing depth. Theoretically the computational requirements double as the compression depth is increased one step forth. Hence, selection of compression depth is a matter of decision based on the available computational power that can be permitted by the real time processing unit under certain sampling time constraint.

B. Experiment Set-2

Another set of experiments is made to observe the relationship between compression ratio and the size (i.e. length) of buffer used for storing and reconstructing the data under constant compression depth for wavelet families Biorthogonal 2.6, Reverse Biorthogonal 2.6, Coiflets 5 and Daubechies 5. Once again reconstruction power error is taken as the major metric to analyze the results which are shown in Fig. 11. In this experiment set, the buffer length used in the algorithm is swept from 16 to 128 and the compression rate is kept at $\%90$ for all wavelet families.

The results obtained from this experiment set show that the reconstruction error decays exponentially as the buffer size is increased. In other words, increasing buffer length after a certain point has almost negligible effect on the overall reconstruction performance of the signal. On the other hand, just like the compression depth, having larger buffer means increased computational cost.

Another important result obtained from Fig. 11 is the considerable change of reconstruction error between wavelet families. For the entire sweep range of buffer size, Bior family outperforms the other wavelet bases while the worst results are obtained from Coiflet family. Having considered the simpler structure of Bior with respect to other families, one can conclude that it comes out as the best selection for the entire range of buffer length.

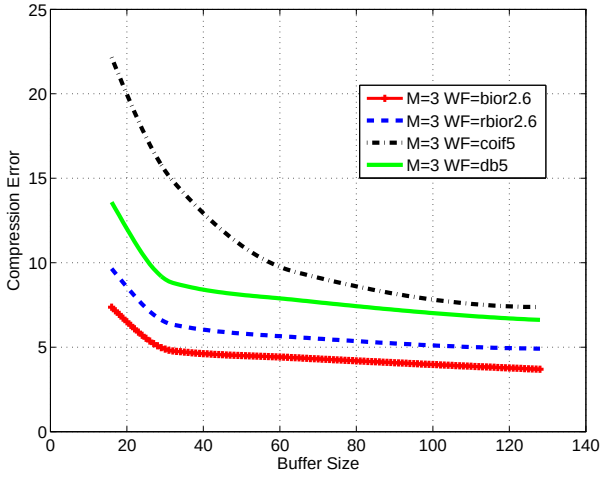

Fig. 11. Comparison of Wavelet Families With Respect to Buffer Size

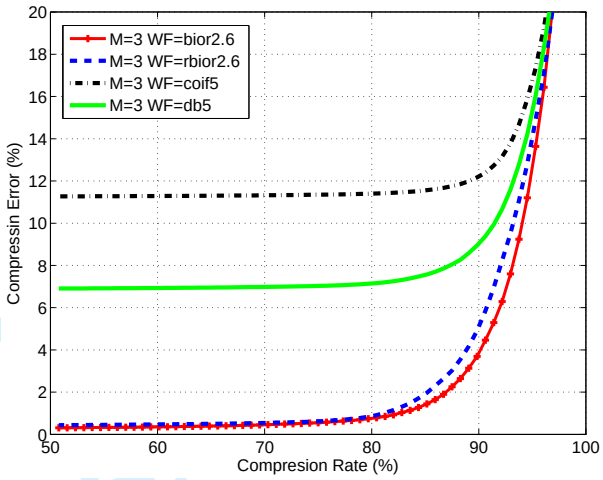

Fig. 12. Comparison of Wavelet Families With Respect to Compression Ratio

C. Experiment Set-3

The final set of experiments includes a comparison between the wavelet families with respect to power error under constant buffer size and constant level of compression. For that purpose, results obtained from families Biorthogonal 2.6, Reverse Biorthogonal 2.6, Coiflets 5, and Daubechies 5 are compared and shown in Fig. 12 all of which having buffer size equal to 128 and compression depth being equal to 3.

Based on the results shown in the figure, one can conclude that in terms of error performance, Bior family once again give the best response while Coiflet family performs worst. Families Rbior and Daubechies show intermediate responses. However, here one can also observe that for low ranges of compression, Rbior family gives almost the same response with Bior bases.

VII. Discussion

Having evaluated the results shown in these experiments, few important conclusions can be summarized. The first result is the negligible effect of vanishing moments on the performance of the system. Since vanishing moments add up with further computational complexity, for realization of the given framework, it is recommended to take the vanishing moments with the least complication. The second remarkable conclusion that can be observed from the system is improvement of performance with increasing compression depth. Based on the results, selection of compression depth at the level $M = 3$ seems to be a good solution as compression rates of $\%85$ can be achieved within the error bounds of $\%5$ with relatively low computational requirement. Another result obtained from the experiments indicate that increasing buffer size contributes on the reconstruction performance in an exponentially decaying manner. On the other hand like the vanishing moments and compression depth, buffer size also negatively affects the computational requirements of the system. As the computational requirements increase linearly with increasing buffer size, one can make a relatively easier selection. From the given results, a buffer size of 64 seems to be a good selection for bilateral control application. The final result that can be acquired from the last experiment set indicates that the reconstruction error remains same for most of the range of compression ratios. However, increasing the compression ratio beyond values of $\%80$, the power error starts to rise up exponentially with compression rate for all families. Having summarized all these results, a meaningful selection of the system configuration for the proposed WPT based compression scheme will be using the basis family Bior2 with the first vanishing moment (i.e. Bior2.2) and with compression depth of $M = 3$ and buffer size of 64.

In order to better illustrate the performance of the compression algorithm, the position responses of the master and slave manipulators are recorded and shown in this section. For that purpose, the master system is operated under a computer controlled sinusoidal position reference and the compressed control current is sent to the slave system over an artificially generated network delay of varying magnitude between $95ms$ and $105ms$. Following the discussion on the results obtained from experiments, the WPT based compression algorithm is tuned to have the configuration described at the end of the previous paragraph. The decompressed control signal is then used to drive the slave system based on the time delayed motion control algorithm described in Section II. In order to observe the performance of the proposed codec scheme in real time control, the original master position signal is also transferred through the same amount of delay and plotted together with the actual slave position response under the label "Ideal Slave" as shown in Fig. 13 below.

As obvious from the given plots, the proposed WPT based algorithm performs efficiently in compressing and decompressing the high frequency signals being used in network delayed teleoperation systems. For the sake of completeness,

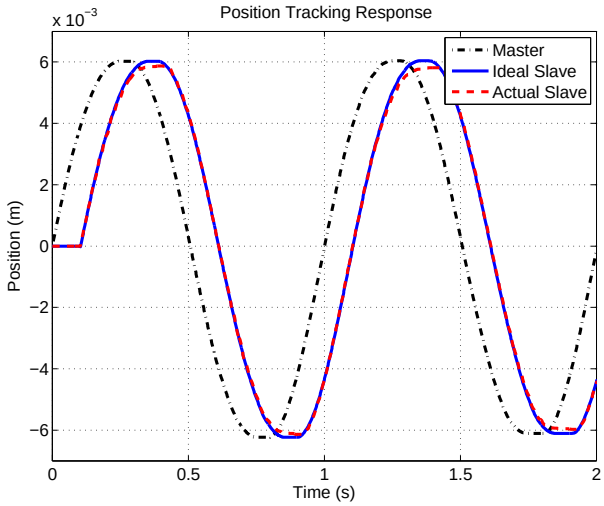

Fig. 13. Position Tracking Responses of the Master and Slave Systems

the actual slave motion data is analyzed in terms of power error with respect to the ideal slave motion data using the power error defined in equation (19). It turns out that the power error between ideal and actual slave motion is $\%4.81$ meaning that the recovery of original data is made with an accuracy level above $\%95$. It should also be pointed out here that this error contains both the error due to the imperfections of estimation in network delayed control algorithm (Section II) and the error due to compression and decompression in WPT based algorithm. Hence, the proposed algorithm alone is supposed to perform even better if all imperfections in the system are cleared out.

VIII. Conclusion

In this study, a compression-decompression algorithm using Wavelet Packet Transform is proposed as a novel approach for bilateral control systems targeted to be used for teleoperation. The derivation of the proposed codec scheme is followed by detailed analysis of the factors and parameters affecting the performance of the system. For convenience of the reader, brief summaries of the controller structure and the wavelet families that are used in the context of this study are provided. Detailed experimental results are evaluated in a comparative manner and several conclusions are drawn to utilize the algorithm in teleoperation with the best possible performance.

Acknowledgment

The authors would gratefully acknowledge the TUBITAK Projects 111M359 and 110M425 and TUBITAK-Bideb for the financial support.

References

[1] Heemels WH, Teel AR, van de Wouw N, Nesic D. Networked control systems with communication constraints: Tradeoffs between transmission intervals, delays and performance. Automatic Control, IEEE Transactions on. 2010;55(8):1781–1796.

[2] Yashiro D, Ohnishi K. Performance analysis of bilateral control system with communication bandwidth constraint. Industrial Electronics, IEEE Transactions on. 2011;58(2):436–443.

[3] Smith OJ. A controller to overcome dead time. ISA Journal. 1959;6(2):28–33.

[4] Anderson R, Spong MW. Bilateral control of teleoperators with time delay. Automatic Control, IEEE Transactions on. 1989;34(5):494–501.

[5] Ryu JH, Kwon DS, Hannaford B. Stable teleoperation with time-domain passivity control. Robotics and Automation, IEEE Transactions on. 2004;20(2):365–373.

[6] Ryu JH, Preusche C. Stable bilateral control of teleoperators under time-varying communication delay: Time domain passivity approach. In: Robotics and Automation, 2007 IEEE International Conference on. IEEE; 2007. p. 3508–3513.

[7] Niemeyer G, Slotine JJ. Stable adaptive teleoperation. Oceanic Engineering, IEEE Journal of. 1991;16(1):152–162.

[8] Niemeyer G, Slotine JJE. Telemanipulation with time delays. The International Journal of Robotics Research. 2004;23(9):873–890.

[9] Daly JM, Wang DW. Time-delayed bilateral teleoperation with force estimation for n-dof nonlinear robot manipulators. In: Intelligent Robots and Systems (IROS), 2010 IEEE/RSJ International Conference on. IEEE; 2010. p. 3911–3918.

[10] Love LJ, Book WJ. Force reflecting teleoperation with adaptive impedance control. Systems, Man, and Cybernetics, Part B: Cybernetics, IEEE Transactions on. 2004;34(1):159–165.

[11] Lawrence DA. Stability and transparency in bilateral teleoperation. Robotics and Automation, IEEE Transactions on. 1993;9(5):624–637.

[12] Natori K. Time Delay Compensation for Motion Control Systems. Keio University, Yokohama, Japan; 2008.

[13] Natori K, Oboe R, Ohnishi K. Analysis and design of time delayed control systems with communication disturbance observer. In: Industrial Electronics, 2007. ISIE 2007. IEEE International Symposium on. IEEE; 2007. p. 3132–3137.

[14] Natori K, Tsuji T, Ohnishi K. Time delay compensation by communication disturbance observer in bilateral teleoperation systems. In: Advanced Motion Control, 2006. 9th IEEE International Workshop on. IEEE; 2006. p. 218–223.

[15] Šabanović A, Ohnishi K, Yashiro D, Šabanović N, Baran EA. Sustavi upravljanja gibanjem s komunikacijskim kašnjenjem. AUTOMATIKA: časopis za automatiku, mjerenje, elektroniku, računarstvo i komunikacije. 2010;51(2):119–126.

[16] Sabanovic A, Ohnishi K, Yashiro D, Sabanovic N. Motion control systems with network delay. In: Industrial Electronics, 2009. IECON'09. 35th Annual Conference of IEEE. IEEE; 2009. p. 2277–2282.

[17] Willaert B, Reynaerts D, Van Brussel H, Vander Poorten EB. Bilateral Teleoperation: Quantifying the Requirements for and Restrictions of Ideal Transparency. Control Systems Technology, IEEE Transactions on. 2014 Jan;22(1):387–395.

[18] Rodriguez-Seda EJ, Lee D, Spong MW. An experimental comparison study for bilateral internet-based teleoperation. In: Computer Aided Control System Design, 2006 IEEE International Conference on Control Applications, 2006 IEEE International Symposium on Intelligent Control, 2006 IEEE. IEEE; 2006. p. 1701–1706.

[19] Sankaranarayanan G, Hannaford B. Experimental comparison of internet haptic collaboration with time-delay compensation techniques. In: Robotics and Automation, 2008. ICRA 2008. IEEE International Conference on. IEEE; 2008. p. 206–211.

[20] Hokayem PF, Spong MW. Bilateral teleoperation: An historical survey. Automatica. 2006;42(12):2035–2057.

[21] Mizuochi M, Ohnishi K. Coding and decoding scheme for wide-band bilateral teleoperation. In: Advanced Motion Control (AMC), 2012 12th IEEE International Workshop on. IEEE; 2012. p. 1–6.

[22] Kuschel M, Kremer P, Buss M. Passive haptic data-compression methods with perceptual coding for bilateral presence systems. Systems, Man and Cybernetics, Part A: Systems and Humans, IEEE Transactions on. 2009;39(6):1142–1151.

[23] Lee Jy, Payandeh S. Performance evaluation of haptic data compression methods in teleoperation systems. In: World Haptics Conference (WHC), 2011 IEEE. IEEE; 2011. p. 137–142.

[24] Yokokura Y, Katsura S, Ohishi K. Bilateral control using compressor/decompressor under the low-rate communication network. In: Mechatronics, 2009. ICM 2009. IEEE International Conference on. IEEE; 2009. p. 1–6.

[25] Tanaka H, Ohnishi K. Haptic data compression/decompression using DCT for motion copy system. In: Mechatronics, 2009. ICM 2009. IEEE International Conference on. IEEE; 2009. p. 1–6.

[26] Tanaka H, Ohnishi K, Nishi H. Implementation of lossy haptic data compression using integer DCT to FPGA. In: IECON 2010-36th Annual Conference on IEEE Industrial Electronics Society. IEEE; 2010. p. 1726–1731.

[27] Yokokura Y, Katsura S, Ohishi K. Bilateral control using compressor/decompressor under the low-rate communication network. In: Mechatronics, 2009. ICM 2009. IEEE International Conference on. IEEE; 2009. p. 1–6.

[28] Kuzu A, Baran EA, Bogosyan S, Gokasan M, Sabanovic A. WPT based compression for bilateral control. In: Industrial Electronics Society, IECON 2013-39th Annual Conference of the IEEE. IEEE; 2013. p. 5686–5691.

[29] Kuzu A, Baran EA, Bogosyan S, Gokasan M, Sabanovic A. Performance comparison of compression techniques used in bilateral control. In: Industrial Electronics Society, IECON 2013-39th Annual Conference of the IEEE. IEEE; 2013. p. 5674–5679.

[30] Tanaka H, Ohnishi K, Nishi H. Implementation of lossy haptic data compression using integer DCT to FPGA. In: IECON 2010-36th Annual Conference on IEEE Industrial Electronics Society. IEEE; 2010. p. 1726–1731.

[31] Ohnishi K, Shibata M, Murakami T. Motion control for advanced mechatronics. Mechatronics, IEEE/ASME Transactions on. 1996;1(1):56–67.

[32] Saglam CO, Baran EA, Nergiz AO, Sabanovic A. Model following control with discrete time SMC for time-Delayed bilateral control systems. In: Mechatronics (ICM), 2011 IEEE International Conference on. IEEE; 2011. p. 997–1002.

[33] Baran EA, Sabanovic A. Predictive input delay compensation for motion control systems. In: Advanced Motion Control (AMC), 2012 12th IEEE International Workshop on. IEEE; 2012. p. 1–6.

[34] Yu J, Karlsson S. Local spectral analysis using wavelet packets. Circuits, Systems and Signal Processing. 2001;20(5):497–528.

[35] Li Y, Wei Hl, Billings SA. Identification of time-varying systems using multi-wavelet basis functions. Control Systems Technology, IEEE Transactions on. 2011;19(3):656–663.

[36] Wei D, Bovik AC, Evans BL. Generalized coiflets: a new family of orthonormal wavelets. In: Signals, Systems & Computers, 1997. Conference Record of the Thirty-First Asilomar Conference on. vol. 2. IEEE; 1997. p. 1259–1263.

[37] Mallat SG. A theory for multiresolution signal decomposition: the wavelet representation. Pattern Analysis and Machine Intelligence, IEEE Transactions on. 1989;11(7):674–693.

[38] Lee B. Application of the discrete wavelet transform to the monitoring of tool failure in end milling using the spindle motor current. The International Journal of Advanced Manufacturing Technology. 1999;15(4):238–243.

[39] Beylkin G, Coifman R, Rokhlin V. Fast wavelet transforms and numerical algorithms I. Communications on pure and applied mathematics. 1991;44(2):141–183.

[40] Shen J, Strang G. Asymptotics of daubechies filters, scaling functions, and wavelets. Applied and Computational Harmonic Analysis. 1998;5(3):312–331.

[41] Daubechies I. Orthonormal bases of compactly supported wavelets. Communications on pure and applied mathematics. 1988;41(7):909–996.

[42] Cohen A, Daubechies I, Feauveau JC. Biorthogonal bases of compactly supported wavelets. Communications on pure and applied mathematics. 1992;45(5):485–560.

[43] Karam J. On the Zeros of Daubechies Orthogonal and Biorthogonal Wavelets. Applied Mathematics. 2012;3(7).

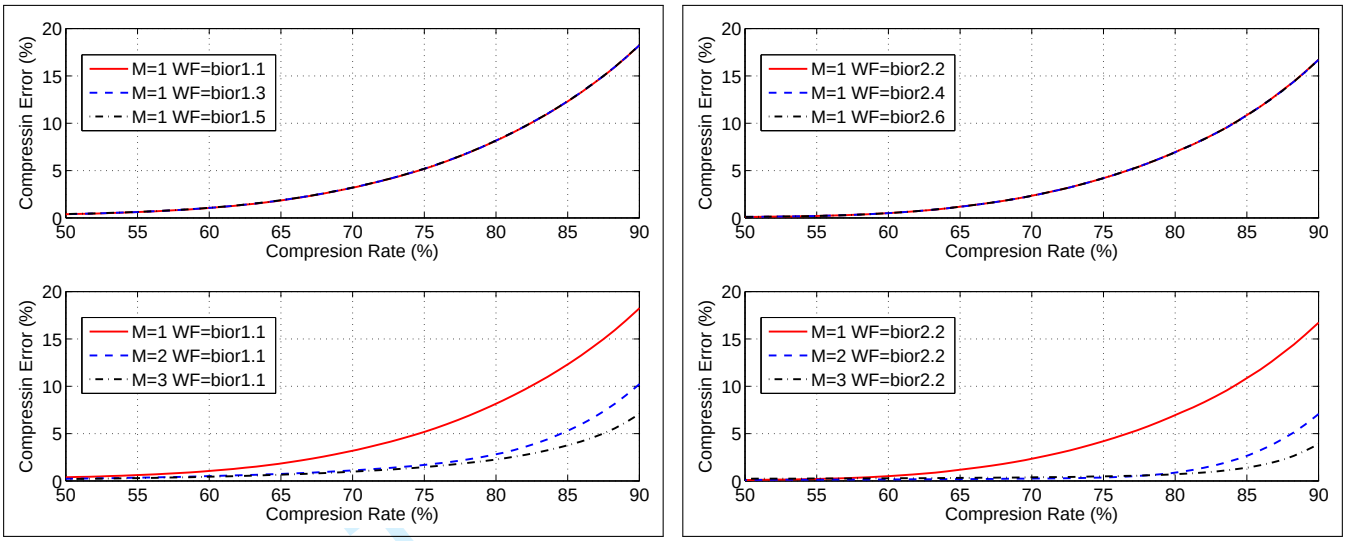

(a) bior1.x

(b) bior2.x

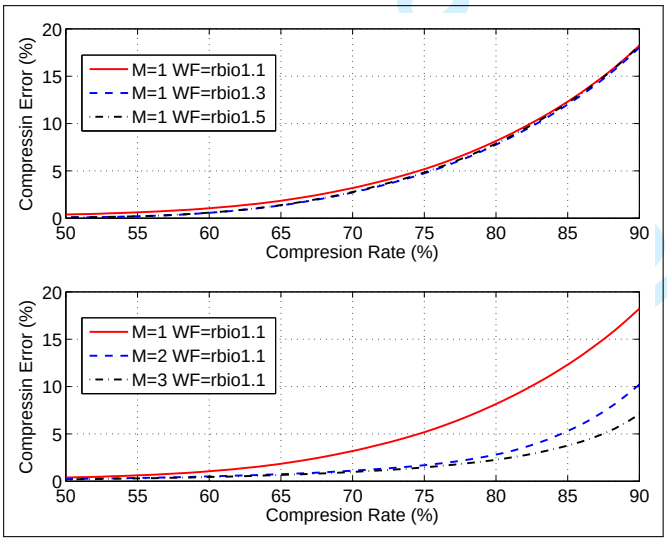

(c) rbior1.x

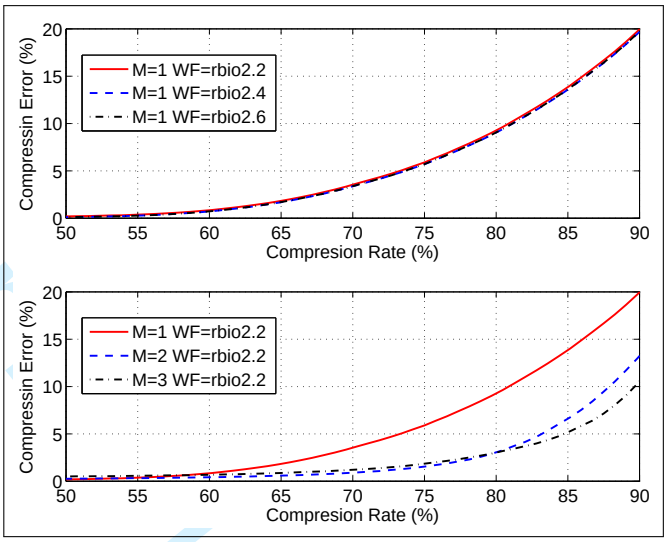

(d) rbior2.x

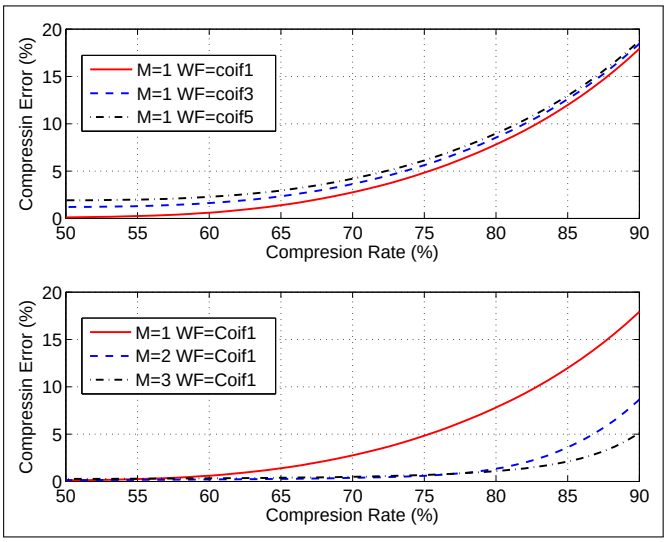

(e) coif

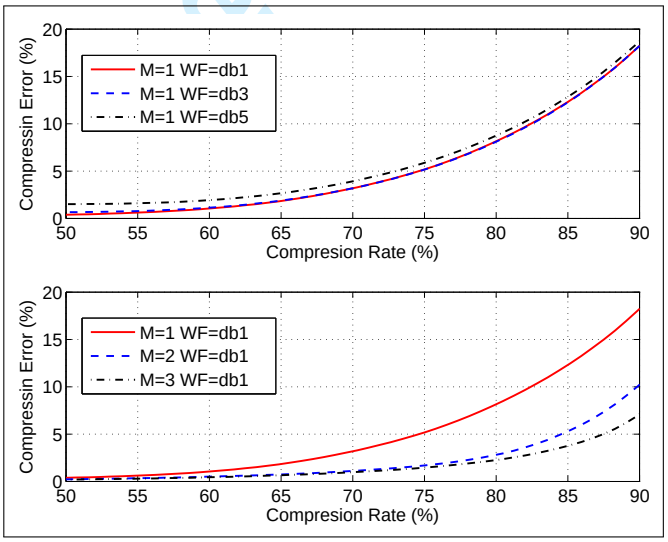

(f) db & haar(db1)

Fig. 10. Comparison of Wavelet Families With Respect to Vanishing Moments and Compression Levels